

# Ordering Fullerenes at the Nanometer Scale on Solid Surfaces

Luis Sánchez,<sup>†</sup> Roberto Otero,<sup>‡,§</sup> José María Gallego,<sup>||</sup> Rodolfo Miranda,<sup>\*,‡,§</sup> and Nazario Martín<sup>\*,†,§</sup>

*Departamento de Química Orgánica, Facultad de C.C. Químicas, Universidad Complutense de Madrid, 28040 Madrid, Departamento de Física de la Materia Condensada, Universidad Autónoma de Madrid, Cantoblanco, 28049 Madrid, Instituto Madrileño de Estudios Avanzados en Nanociencia, IMDEA-Nanociencia, 28049 Madrid, and Instituto de Ciencia de Materiales de Madrid, Consejo Superior de Investigaciones Científicas, Cantoblanco, 28049 Madrid, Spain*

Received July 30, 2008

## Contents

1. Introduction	2081
2. Substrate-Controlled Adsorption of Fullerenes on Solid Surfaces	2083
2.1. Adsorption Site Selectivity	2083
2.1.1. Zero-Dimensional Point Defects: Points of Emergence of Ordered Surface Dislocation Networks	2083
2.1.2. One-Dimensional (1D) Line Defects: Ordered Monatomic Steps on Vicinal Surfaces	2083
2.1.3. One-Dimensional Line Defects: fcc vs hcp Stacked Surface Regions on Au(111)	2084
2.2. Interaction-Controlled Molecular Ordering: Adding Functionality to Fullerenes	2084
2.3. Fullerene Ordering on Nanostructured Surfaces	2085
2.4. Orientational Ordering Imposed by the Substrate	2086
3. Fullerene Adsorption on Surface Scaffoldings by Organic Templates. Formation of 2D Architectures	2086
4. Coadsorbed Fullerene Systems and the Formation of Intermixed Layers at a Nanometer Scale	2088
5. Outlook	2090
6. Acknowledgments	2090
7. References	2090



Dr. Luis Sánchez received his Ph.D. in organic chemistry in 1997 from the Universidad Complutense de Madrid (UCM; Spain) under the supervision of Prof. N. Martín and C. Seoane. In 1998, he joined the faculty at the Department of Organic Chemistry at UCM and was promoted to Associate Professor in 2002. During 1999–2000, he was a postdoctoral researcher with Prof. Jan C. Hummelen (University of Groningen, The Netherlands). His current research interests are focused on new supramolecular ensembles in the study of electron-transfer processes and photovoltaic applications.



Dr. Roberto Otero received his Ph.D. degree from Universidad Autónoma de Madrid in 2002 under the supervision of Prof. Rodolfo Miranda. He then moved to the University of Aarhus, Denmark, where he worked as a postdoctoral assistant in the group of Prof. Flemming Besenbacher. He is presently a Ramón & Cajal Associate Professor at Universidad Autónoma de Madrid. His current research interests focus on the study of the growth and self-assembly of organic adsorbates on solid surfaces by means of scanning tunneling microscopy.

## 1. Introduction

The coverage of solid surfaces with atoms and, more recently, with (organic) molecules is a broad scope area that has received the attention of the scientific community during recent years. This interest is based on the fact that the presence of the (organic) molecules usually modifies the surface properties, resulting in new materials with enhanced properties suitable for the preparation of devices in molecular electronics or for the study of emerging nanoscience and nanotechnology.<sup>1</sup>

In this regard, the design and development of coated surfaces showing unprecedented optoelectronic properties require detailed understanding of the phenomena occurring at the atomistic scale at the interface between the solid surface and the added molecules.<sup>2</sup> To unravel the fascinating

\* To whom correspondence should be addressed. E-mail: rodolfo.miranda@uam.es (R.M.) and nazmar@quim.ucm.es (N.M.).

<sup>†</sup> Universidad Complutense de Madrid.

<sup>‡</sup> Universidad Autónoma de Madrid.

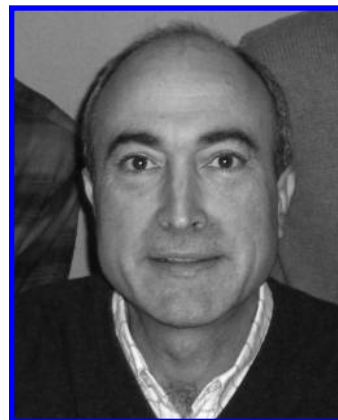
<sup>§</sup> IMDEA-Nanociencia.

<sup>||</sup> Consejo Superior de Investigaciones Científicas.

aspects occurring in these new materials, a wide variety of studies have been carried out on different solid substrates using a huge number of molecules to interact with them. Thus, important topics such as those devoted to nanopar-



Dr. José María Gallego received his B.S. degree in physics from the Universidad Autónoma de Madrid in 1986 and completed his Ph.D. in 1991 with Prof. Rodolfo Miranda. He continued his postdoctoral studies with Prof. Ivan K. Schuller at the Universidad de San Diego, California, before joining the Spanish Consejo Superior de Investigaciones Científicas (CSIC) in 1996 as a tenured scientist. His research interest is centered on the physics of surfaces, thin films, and metallic superlattices, in particular STM studies of the epitaxial growth, in ultrahigh vacuum, of both organic and inorganic materials on solid surfaces.



Prof. Nazario Martín is a full professor at the University Complutense of Madrid (UCM). He worked as a postdoctoral fellow (1987–1988) at the Universität Tübingen with Michael Hanack on electrically conducting organic materials. In 1994, he was a visiting Professor at the University of California, Santa Barbara (UCSB), working with Fred Wudl on fullerenes, and in 2005 at the Universities of California, Los Angeles (UCLA), and Angers (France). Professor Martín's research interests include the chemistry of carbon nanostructures,  $\pi$ -conjugated systems, and electroactive molecules in the context of electron transfer processes, photovoltaic applications, and nanoscience. He is a Fellow of the Royal Society of Chemistry and the President of the Spanish Royal Society of Chemistry.



Prof. Rodolfo Miranda received his B.S. degree from the Universidad Autónoma de Madrid (UAM) in 1975 and a Ph.D. in Physics from UAM in 1980. He worked in Munich and Berlin with Gerhard Ertl (NL in Chemistry 2007) before he was appointed Full Professor of Condensed Matter Physics at the UAM in 1992. He is a Fellow of the American Physical Society. His research interests include the application of scanning tunneling microscopy in ultra high vacuum conditions to epitaxial growth, quantum size effects, nanomagnetism, and functional molecules.

ticles,<sup>3</sup> nanoelectrodes and nanopores,<sup>4</sup> self-assembling monolayers (SAMs) and multilayers,<sup>5</sup> the most recent so-called “nanovehicles”,<sup>6</sup> or, for instance, dendrimers at the nanometer scale for application in molecular electronics, sensing, or catalysis<sup>7</sup> are topics where the topological and electronic interactions occurring at the interface between the substrate and the molecules are critical.

Needless to say, to have good expertise in all of these topics as well as in their applications, such as light conversion,<sup>8</sup> or to discuss their manipulations (electric measurements and charge transport,<sup>9</sup> nanocars,<sup>10</sup> etc.) is out of the scope of a single research group; therefore, multidisciplinary studies are required for the rational development and applications of these modified surfaces.

In this context, the coverage of solid surfaces with fullerenes offers the possibility of transferring the fascinating properties of these molecular carbon allotropes (involving chemical, electrochemical, and photophysical properties) to solid surfaces.<sup>11</sup> The chemical and physical methods available

allow transfer of fullerenes in a controlled way to the substrate, giving rise to ordered structures where electronic interactions between the molecules with the solid surface or with other closed molecules are responsible for the two-dimensional (2D) supramolecular organizations.

Fullerenes are fascinating spherical molecules exhibiting outstanding chemical, electrochemical, and photophysical properties, which have made them one of the most studied chemical compounds during the last 20 years.<sup>12</sup> As a result, nowadays, there is a good understanding of the covalent chemistry of these carbon allotropes.<sup>13</sup> Supramolecular chemistry of fullerenes has also been developed to a great extent, and because of their singular geometry, these spherical molecules have been used as both hosts and guests in a wide variety of supramolecular ensembles reported during the last years.<sup>14</sup>

A different supramolecular approach to that known in solution or three-dimensional (3D) crystals, which currently represents a major challenge in science, is the engineering of atoms or (organic) molecules on atomically well-defined solid surfaces of a different nature, mainly involving metals (Au, Cu, or Ag) or semimetals (graphite). The aim is to achieve good control of the self-ordering of the adsorbed atoms or molecules on the substrate with the final goal of obtaining new nanostructured functional materials for the preparation of smaller devices.<sup>15</sup> This bottom-up approach, which is mainly based in the characterization of samples by using modern microscopy techniques [scanning tunneling microscopy (STM), atomic force microscopy (AFM), and transmission electron microscopy (TEM)], requires a good understanding of the interactions occurring between the substrate and the adsorbed molecules as well as the ones among the molecules in the presence of the interacting solid surface. Thus, the 2D arrangement is a result of a combination of weak noncovalent intermolecular forces (such as van der Waals or dispersive forces) with molecule–substrate interactions, where crystalline symmetry of the surface plays a leading role.<sup>16</sup> Therefore, supramolecular chemistry is an important tool for the development and understanding of the emergent nanoscience and nanotechnology at surfaces.

In this regard, molecule–substrate interactions usually determine adsorption geometry and conformation at low surface coverages. Only when molecules are able to form strong directional bonds, such as H-bonds, and the corrugation of the potential energy for the adsorbed species is small as compared to the energy gain from intermolecular interactions, supramolecular structures formed on surfaces are mainly determined by intermolecular forces (although the substrate influence may still be important).<sup>17</sup> On the other hand, in some specific systems—such as the Au(111) surface—there is a strong selectivity in the adsorption site of the adsorbates, which, in turn, determines the final morphology of the organic monolayer.

Herein, we review the different strategies followed for the incorporation of fullerene molecules onto solid surfaces, which mainly involve (i) the site-selective adsorption of fullerene or fullerene derivatives on a bare metal—where reconstructions frequently occur on the metal surface—or semiconductor surface; (ii) the generation of a regular network of an organic molecule on the surface, which, in turn, is used as a template for the further controlled organization of fullerenes, thus avoiding the strong tendency of fullerenes to rearrange the substrate atomic structure; and (iii) the formation of lateral superlattices at a nanometer scale by mixing fullerenes with other electronically complementary molecules.

The aim of this review is not to make a comprehensive presentation of the still relatively few examples known on surface-supported 2D supramolecular networks involving fullerenes but to show some paradigmatic cases that illustrate the importance of this bottom-up approach for the controlled generation of ordered carbon nanostructures.

## 2. Substrate-Controlled Adsorption of Fullerenes on Solid Surfaces

The nature of the interaction between fullerenes and metal single crystals surfaces has been the subject of a numbers of reports. Recently, Tamai, Baumberger, and co-workers have addressed the unraveling of the electronic structure at the C<sub>60</sub>/metal interface by means of high-resolution angle-resolved photoemission,<sup>18</sup> revealing the presence of an extra photoemission peak dispersing in the highest occupied molecular orbital (HOMO)—lowest unoccupied molecular orbital (LUMO) gap, which has been interpreted as a signature of a strong hybridization between the copper and the carbon electronic states. The covalent interaction between C<sub>60</sub> molecules and metallic surfaces is also supported by STM studies—showing a significant influence of the underlying metal on the electronic structure of the adsorbed C<sub>60</sub><sup>19,20</sup>—and DFT calculations.<sup>21</sup> Apart from the hybridization between the *d*-states of the metal surface and the  $\pi$ -orbitals at the C<sub>60</sub> cage, a significant charge transfer from the substrate to C<sub>60</sub> is usually observed, with reported values ranging from 0.7 to 2 *e*/C<sub>60</sub>.<sup>22</sup>

Another topic that has been amply discussed in the literature is the effect of surface reconstruction upon fullerene adsorption. For strongly interacting substrate/adsorbate systems, adsorption often leads to significant changes in the subtle energetic balance governing surface structure and, thus, to a significant modification of the substrate's atomic geometry known as surface reconstruction. For fullerene adsorption on clean metal surfaces, surface reconstruction seems to be the rule rather than the exception. For example, Pd(110)<sup>23</sup> and Ni(110)<sup>24</sup> surfaces show large mass transport

associated with fullerene adsorption; the strong interaction between these *d*-band metals and the  $\pi$ -systems of C<sub>60</sub> promotes the creation of a long-range ordered array of vacancy islands that permit a closer interaction between the metal surface and the lateral  $\pi$ -electrons of the C<sub>60</sub> cage that otherwise would not be in close proximity of any surface atoms. There is even ample evidence supporting surface reconstruction for the much less reactive noble metal surfaces,<sup>25–28</sup> including close-packed ones.<sup>29–31</sup>

### 2.1. Adsorption Site Selectivity

#### 2.1.1. Zero-Dimensional Point Defects: Points of Emergence of Ordered Surface Dislocation Networks

Surfaces showing well-ordered, uniform arrays of anchoring sites are excellent templates for the preparation of ordered molecular nanostructures by site-selective nucleation and a further self-assembly of the adsorbed molecules. This has been shown for metallic nanostructures, for example, as a consequence of the strain-relief patterns and dislocation networks characteristics of some solid surfaces, for example, the Au(111) herringbone-reconstructed surface,<sup>32</sup> which favors the initial nucleation in preferential regions.<sup>33</sup> Actually, a wide variety of surface defects, such as steps or impurities, can also act as nucleation sites for anchoring molecules. While, contrary to metal adatoms,<sup>34</sup> C<sub>60</sub> molecules have *not* been observed to decorate preferentially the elbows of the herringbone reconstruction, fullerene derivatives, such as PCBM (phenyl-C<sub>61</sub>-butiric acid methyl ester),<sup>35</sup> adsorb preferentially at the elbows, forming a regular array of single molecules (Figure 1).<sup>36</sup> At low coverages, because of the influence of the “side-tail” of PCBM, the herringbone reconstruction of Au(111) acts, thus, as an efficient template that dictates the resulting structure.<sup>36</sup>

#### 2.1.2. One-Dimensional (1D) Line Defects: Ordered Monatomic Steps on Vicinal Surfaces

Fullerenes have been deposited onto metal surfaces since the early 1990s, and in particular, the most studied C<sub>60</sub> molecule has been observed to diffuse fast on Au(111) 22 × √3 herringbone-reconstructed surfaces at room temperature, to end up being selectively anchored at the lower step edges on the face-centered cubic (fcc) areas.<sup>37</sup> This observation suggested the possibility to employ vicinal Au surfaces with a periodic arrangement of monatomic steps as a template to obtain ordered arrays of fullerene molecules. In stepped and reconstructed gold surfaces [vicinal to the (111) face], a rectangular array of preferred adsorption sites arises from the perpendicular intersection of two nanoscale patterns of different origin: step edges and dislocation lines from the remaining herringbone reconstruction on the (111) facets.

This inherent property of vicinal gold surfaces has been skillfully exploited by Fasel and co-workers for preparing C<sub>60</sub> nanostructures with long-range order and uniform size by using Au(11 12 12) surfaces, which consists of 7 nm wide (111)-oriented terraces separated by a periodic array of (100) monatomic steps.<sup>38</sup> After deposition of 0.1 monolayer (ML) of C<sub>60</sub> on the gold surface at room temperature, a highly regular 2D superlattice of short molecular chains, formed mostly by four or five C<sub>60</sub> units, was observed (Figure 2). Interestingly, the nanochain superlattice contains fullerene molecules adsorbed exclusively on the fcc areas of the step edges of the substrate.<sup>38</sup> This organization has been accounted

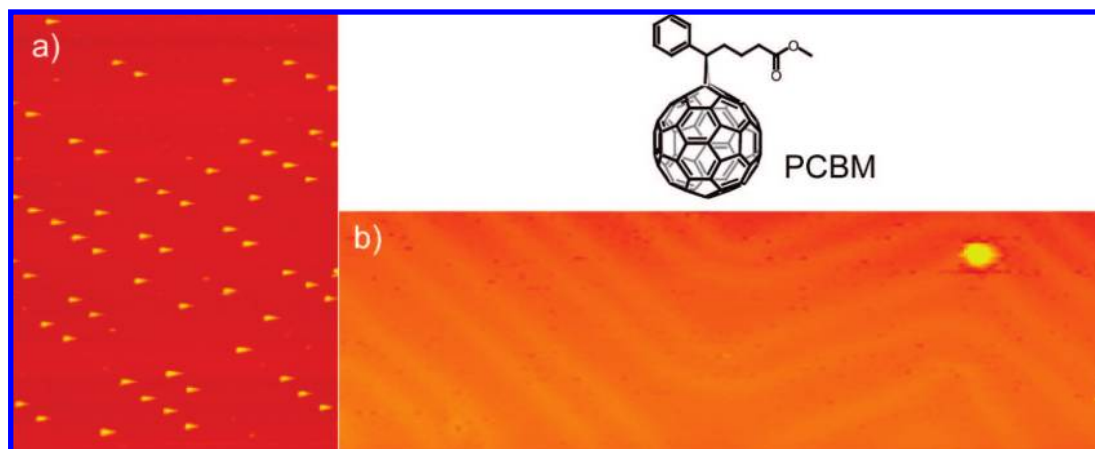


**Figure 1.** (a) STM image ( $92 \times 127 \text{ nm}^2$ ) of a highly regular 2D array of the  $\text{C}_{60}$  derivative PCBM molecules on the reconstructed Au(111) template surface. (b) High-resolution image of a single PCBM molecule adsorbed at the elbow of the herringbone reconstruction.

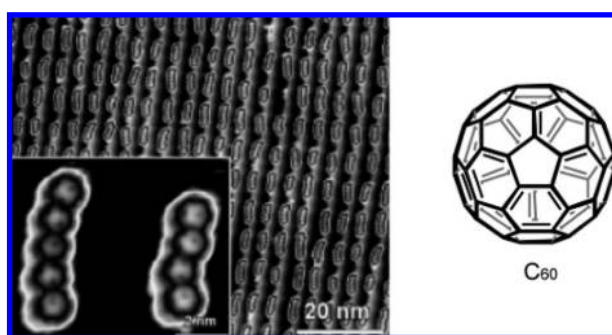


**Figure 2.** STM image of the superlattice obtained after formation of a highly regular 2D array of  $\text{C}_{60}$  nanochains on the Au(111212) template surface after deposition of  $\sim 0.1 \text{ ML}$  of  $\text{C}_{60}$  ( $T \sim 40 \text{ K}$ ,  $V_{\text{bias}} = -2 \text{ V}$ , and  $I_s = 0.03 \text{ nA}$ ). The inset ( $V_{\text{bias}} = -2.5 \text{ V}$ , and  $I_s = 0.5 \text{ nA}$ ) shows a high-resolution image of two short chains. Reproduced with permission from ref 38. Copyright 2006 American Chemical Society.

for by the possibility of a certain charge transfer degree from the electron-rich step edge to the electron deficient  $\text{C}_{60}$ . Only after complete decoration of the step edges, close-packed  $\text{C}_{60}$  islands grow. At higher coverages, the  $\text{C}_{60}$  layer grows out from the chains and across the terraces, which is energetically favored over the closing of the nanochain segments into extended 1D molecular chains.

Berndt's group has used the tendency toward faceting of the Au (433) vicinal surface—with regular 4 nm wide terraces separated by bunches of 1.4 nm terraces—and the trend of  $\text{C}_{60}$  to modify the atomic structure of some metal surfaces to fabricate long and narrow fullerene stripes. The combination of  $\text{C}_{60}$  adsorption on the gold vicinal surface and subsequent annealing to 500 K results in the formation of a faceted surface decorated with alternating metal and fullerene stripes, several hundreds of nanometers long, with an average width of 6–8 adjacent molecular chains (Figure 3).<sup>39</sup>

### 2.1.3. One-Dimensional Line Defects: fcc vs hcp Stacked Surface Regions on Au(111)

Even on flat (nonvicinal) Au(111) surfaces, the dislocation pattern arising from the herringbone reconstruction also provides a 1D template for the growth of fullerene derivatives. For example, in the case of PCBM, the organization process starts with adsorption of individual PCBM molecules at the elbows of the reconstruction as described above but for larger coverage continues with the formation of 1D wires

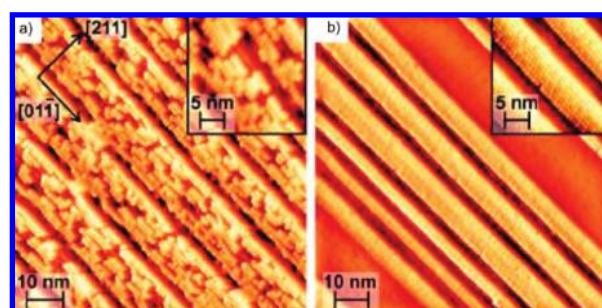


**Figure 3.** STM images of the deposition of 0.5 ML of  $\text{C}_{60}$  on Au(433) before (a) and after (b) annealing at  $T = 500 \text{ K}$  for 15 min. The insets show close-up views. Reproduced with permission from ref 39. Copyright 2006 American Chemical Society.

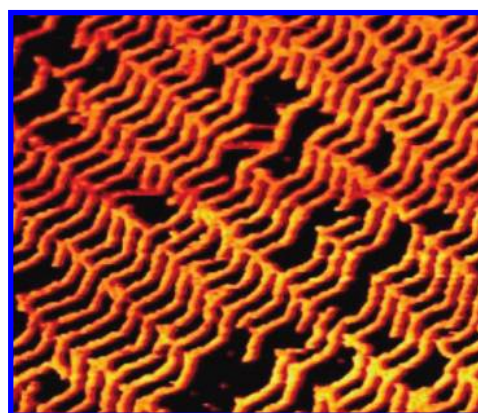


**Figure 4.** STM images of the deposition of 0.5 ML of PCBM on Au(111). Reproduced with permission from ref 36. Copyright 2007 Wiley-VCH Verlag GmbH & Co. KGaA.

formed by double rows of PCBM molecules nucleated exclusively at the fcc areas of the reconstruction, which gives rise to a 2D nanosized spiderweb of PCBM nanowires (Figure 4).<sup>36</sup>

## 2.2. Interaction-Controlled Molecular Ordering: Adding Functionality to Fullerenes

The intrinsically symmetric nature of fullerenes makes difficult their organization in complex structures. This can be achieved by functionalizing fullerene with added specific groups. In a recent study, we have shown that UHV deposition of the fullerene derivative PCBM—which has been

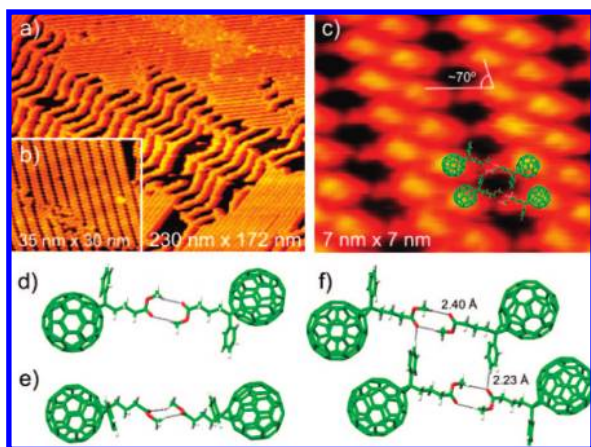


**Figure 5.** Large-scale STM image of the Au(111) surface after depositing  $\sim 0.6$  ML of PCBM, showing the coexistence of two different phases: (a) the nanoscale spiderweb (created by the templating effect of the substrate surface) and (b) the sets of parallel double rows connected by an array of weak hydrogen bonds. (c) Close-up of PCBM double rows produced on Au(111) by the take over of the intermolecular interactions. (d) Top and (e) side views of the optimized (calculated) structure for a PCBM dimer. (f) Optimized structure for a PCBM tetramer. The dotted lines mark the weak hydrogen bonds responsible for this conformation. Reproduced with permission from ref 36. Copyright 2007 Wiley-VCH Verlag GmbH & Co. KGaA.

extensively used in organic photovoltaic solar cells<sup>40</sup>—on Au(111) leads to a coverage-dependent transition from substrate-controlled to (weak) H-bond-controlled self-assembly.<sup>36</sup> As the density of the molecules increases above the coverage for which the nanoscale spiderweb described above is found, the collective effect of the intermolecular interactions (weak hydrogen bonds) lifts the templating effect of the substrate reconstruction, to result in the formation of long, straight wires of double rows of PCBM molecules (Figure 5). These findings reveal that when the density of molecules exceeds that of the available fcc areas, the interactions between the organic addends of the fullerenes take over molecule–substrate interactions, resulting in a cross-over from substrate-controlled to intermolecular interaction-controlled in the surface organization of PCBM molecules.

Density functional theory calculations predict that two PCBM molecules are connected through two weak H-bonds between the tails, leading to an energy gain of 2.19 kcal/mol in comparison with two isolated molecules. A further calculation of the tetramer by considering the presence of two additional H-bonds between adjacent dimers resulted in an excellent agreement with the experimental findings (Figure 5). Interestingly, weak H-bonds of type C–H $\cdots$ O have been a matter of discussion during the last 25 years, being recognized as a key aspect in many supramolecular organizations.<sup>41</sup> In our case, the weak H-bonds between the methyl ester groups and between the phenyl rings and the carbonyl functionalities are responsible for the observed cross-over site selectivity, confirming that they could be a valuable tool for engineering molecular nanostructures at surfaces.

Nanowires of other fullerene derivatives have also been formed in a predictable way on graphite surfaces by using fullerenes with long alkyl chains (compounds **1a–e** in Figure 6).<sup>42</sup> The samples were deposited on highly oriented pyrolytic graphite (HOPG) by spin-coating from chloroform solutions and were then studied by STM at 100 K under UHV conditions. Lamellar structures and 1D alignment of the

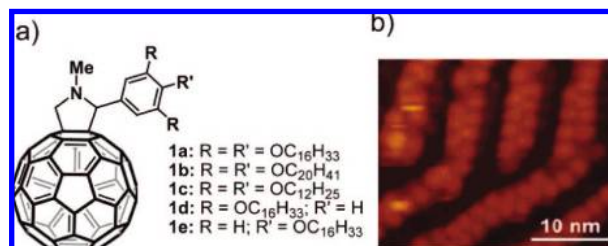


**Figure 6.** (a) Chemical structure of fullerene derivatives **1**. (b) High-resolution STM image of **1a** on HOPG (scan range,  $30 \times 30$  nm<sup>2</sup>;  $I_s = 40$  pA; and  $V_{\text{bias}} = +3.0$  V). Reproduced with permission from ref 42. Copyright 2006 American Chemical Society.

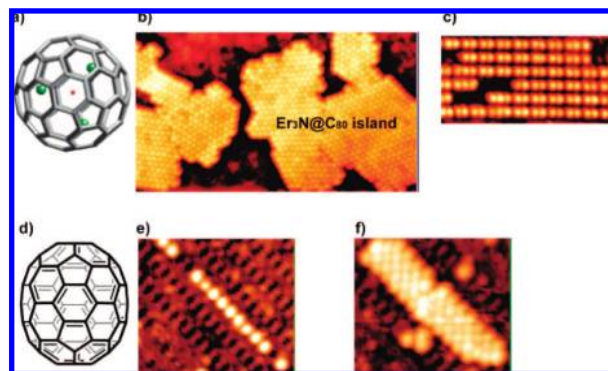


**Figure 7.** Chemical structure of  $\text{Er}_3\text{N}@C_{80}$  (a) and STM images of molecular islands of it on  $\text{SrTiO}_3(001)\text{-c}(4 \times 2)$  ( $55.4 \times 31.3$  nm<sup>2</sup>,  $V_s = +1.6$  V, and  $I_t = 0.10$  nA) (b). Two-dimensional endohedral fullerene array organization ( $31 \times 16$  nm<sup>2</sup>,  $V_s = +3.0$  V, and  $I_t = 0.1$  nA) on  $\text{SrTiO}_3(001)\text{-(}6 \times 8\text{)}$  (c). STM images of the growth of epitaxial  $C_{70}$  (d) islands onto  $\text{SrTiO}_3(001)$  showing a one-molecule wide chain (e) and a four-molecule-wide island of  $C_{70}$  (f). Imaging conditions:  $V_s = +2.6$  V, and  $I_t = 0.10$  nA for image e and  $V_s = +2.3$  V, and  $I_t = 0.10$  nA for image f. Reproduced with permission from ref 43. Copyright 2006 American Chemical Society. Reproduced with permission from ref 44. Copyright 2007 Royal Society of Chemistry.

fullerenes were observed. This study revealed the strong impact that the presence of alkyl chains has on the 2D arrangement. Thus, derivatives bearing three alkyl chains are adsorbed in a head-to-head bilayer structure resulting in zigzag type of wires within the lamellae. In contrast, the presence of only one alkyl chain gives rise to the formation of an interdigitated lamella. The spacing between lamellae is determined by the alkyl chain length.

The interactions described above reveal the important role that supramolecular chemistry can play in the construction of molecular nanostructures on solid surfaces. The arsenal of noncovalent interactions available—where alkyl chains and functional groups can play a leading role—to achieve a rational order of the molecules on the substrate is currently being applied on different solid surfaces and must lead to amazing results in the next coming years.

### 2.3. Fullerene Ordering on Nanostructured Surfaces

Nanostructured  $\text{SrTiO}_3(001)$  has also been used as a template to order endohedral  $\text{Er}_3\text{N}@C_{80}$  and  $C_{70}$  molecules (Figure 7). The adsorption of  $\text{Er}_3\text{N}@C_{80}$  (Figure 7a) on  $\text{SrTiO}_3(001)$  results in the formation of close-packed islands without an apparent epitaxial relationship with the  $c(4 \times 2)$  reconstruction of the surface (Figure 7b). However, preparing the sample with an intensive sputtering and annealing procedure ( $945$  °C and  $>1$  h) yields a different surface

reconstruction, with a periodicity ( $6 \times 8$ ), and subsequent deposition of  $\text{Er}_3\text{N}@C_{80}$  giving rise to a 2D organization as a consequence of the fitting of this endohedral fullerene in the array of monatomic deep trenches generated on the  $\text{SrTiO}_3(001)$  surface (Figure 7c).<sup>43</sup> In contrast,  $C_{70}$  fullerene (Figure 7d) deposited on the standard  $c(4 \times 2)$  reconstruction of  $\text{SrTiO}_3(001)$  forms a number of linear configurations, from one-molecule wide linear chains to two-molecule wide clusters, as well as three-, four-, and five-molecule wide elongated islands (Figure 7e,f). As expected, because of the absence of alkyl chains or functional groups on the fullerene molecule as well as to the large corrugation of this surface, the observed configurations assume a packing order that is commensurate with the substrate. This finding has been accounted for by considering that the locations of the bonding sites are correlated to the size and geometry of the molecules in relation with the size and geometry of the substrate.<sup>44</sup>

## 2.4. Orientational Ordering Imposed by the Substrate

In contrast to most of the planar molecules, which usually adsorb flat on surfaces, spherical fullerenes add an additional rotational degree of freedom and, consequently, a higher level of complexity. STM has been successfully used for detecting the orientation of the  $C_{60}$  units despite their spherical shape. These studies reveal random orientation<sup>45</sup> of the fullerene molecules forming the assembled clusters or monolayers. Only in a few cases the strong interaction between the  $C_{60}$  units and the solid surface results in simple orientational order with a uniform orientation<sup>46</sup> or ordered alternation of two orientations.<sup>47</sup>

In this regard, Berndt's group has recently found a long-range orientational order in a  $C_{60}$  monolayer on Au(111) by using STM at low temperature.<sup>48</sup> Remarkably, a unit cell formed by 49  $C_{60}$  molecules adopts 11 different orientations (Figure 8). This unit cell can be divided into a faulted and an unfaulted half—similar to the  $(7 \times 7)$  reconstruction of Si(111). In this singular case, intermolecular interactions play a leading role in stabilizing the observed superstructure.

## 3. Fullerene Adsorption on Surface Scaffoldings by Organic Templates. Formation of 2D Architectures

While the adsorption and self-assembly of fullerenes on bare metal surfaces could be naturally patterned at the nanoscale by the presence of surface reconstructions or step-edge arrays, they offer very little flexibility with regard to the overall geometry of the nucleation sites. A two-step approach has been tried by different research groups in recent years: In the first step, a monolayer of organic molecules is deposited on the solid surface, which would self-assemble into long-range ordered arrays, thereby providing an organic nanoscale pattern for the subsequent, second step, deposition of fullerenes. This approach allows the rational design of a nanoscaffold by a careful choice of the molecular species involved. Furthermore, these hierarchical arrays allow avoidance of the strong tendency of fullerenes to modify the substrate atomic structure.

Although one of the first papers published on this kind of 2D structures involved calix[8]arene,<sup>49</sup> most frequently, porphyrins are the electron donor molecules used to form supramolecular ensembles by combination with  $C_{60}$  either in solution or in the solid state.<sup>50</sup> The first example of

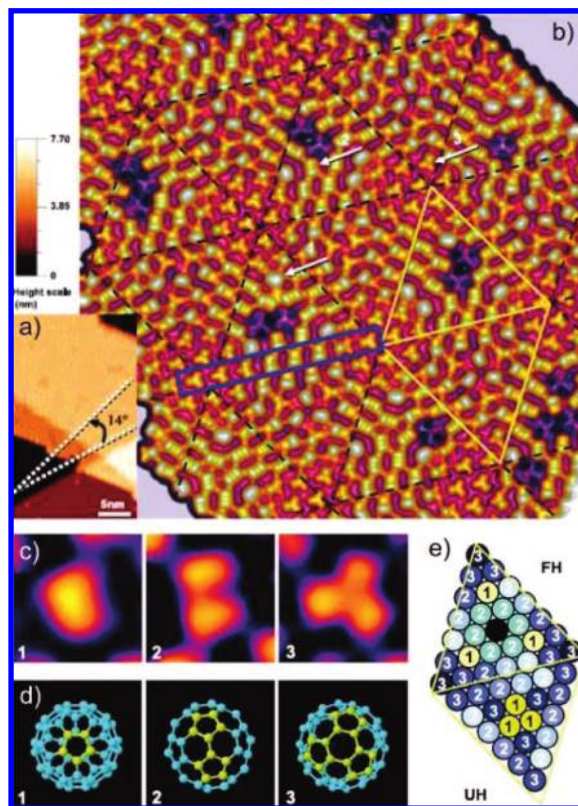


**Figure 8.** STM images ( $I = 0.1$  nA, and  $V = 1.5$  V) of  $C_{60}$  islands deposited at room temperature on Au(111): (a)  $32 \times 20$  nm<sup>2</sup> and (b) pseudo-3D  $20 \times 20$  nm<sup>2</sup>. The height scale corresponds to the highlighted rhombus (a) and (b) defines a unit cell. Added dashed lines indicate equivalent cells. (c) STM images of adsorbed  $C_{60}$  with a 1-, 2-, or 3-fold symmetry axis (1 nm<sup>2</sup>), their corresponding top view models (d), and the proposed  $C_{60}$  arrangement in the superlattice (e). Reproduced with permission from ref 48. Copyright 2007 American Physical Society.

supramolecular architectures formed by assembly of fullerenes and porphyrins on Ag(100) under UHV conditions was recently reported by Spillmann, Jung, Diederich, and co-workers involving compounds **2** and **3** of Figure 9.<sup>51</sup> The self-assembly in these compounds bearing cyanophenyl substituents is due, probably, to both van der Waals and dipole–dipole interactions. STM images at 1 ML coverage reveal that both porphyrins **2** and **3** self-organize in regular molecular rows with a high packing density. The subsequent ordering of deposited  $C_{60}$  molecules depends on the porphyrin structure underneath.

Deposition of 0.14 ML of  $C_{60}$  onto a preadsorbed monolayer of diporphyrin **2** generates unidirectional chains composed of eight  $C_{60}$  molecules (ca. 15.5 nm long and  $4.4 \pm 0.2$  Å high, Figure 9a). These  $C_{60}$  units are located outside of the porphyrin core despite their large surface area. On the contrary, deposition of  $C_{60}$  under the same conditions on a monolayer of **3** on a Ag(111) substrate resulted in the formation of two segregated molecular domains of  $C_{60}$  and **3**, with the  $C_{60}$  units accommodated on top of the porphyrin layer.

Porphyrin **3** has also proven to form a nanoporous phase on Ag(111) that exerts a templating effect in the complexation of  $C_{60}$ . As in the case of bis-porphyrin **2**, STM images of **3** reveal that porphyrins lie flat on the surface without overlapping with their neighbors, forming a hexagonal superstructure of pores with a diameter of  $\sim 1.2$  nm and a depth of  $\sim 1.2$  Å. These pores act as selective receptors for

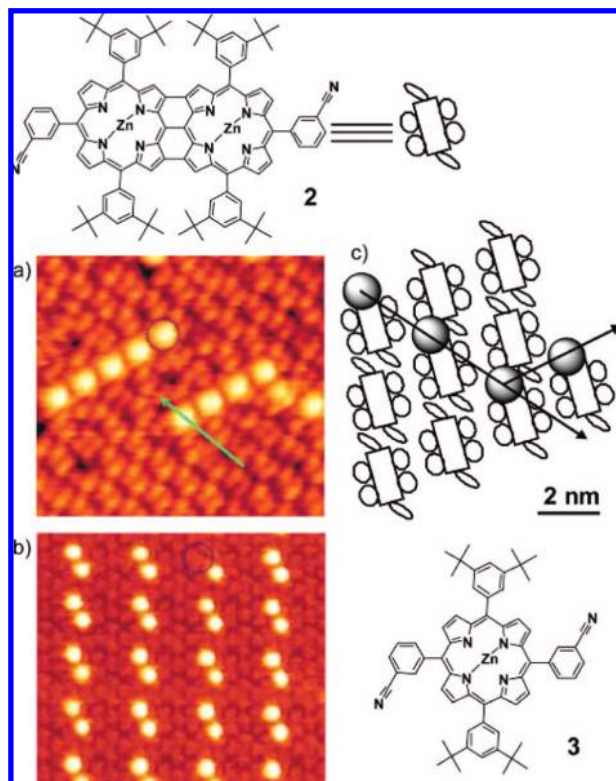


**Figure 9.** Chemical structure of porphyrins **2** and **3** and STM image of  $2 \cdot C_{60}$  (a) and  $3 \cdot C_{60}$  (b) complexes (scan range,  $30 \times 30 \text{ nm}^2$ ;  $I_t = 16 \text{ pA}$ ; and  $V_{\text{bias}} = 2.67 \text{ V}$ ). (c) Proposed model for the assembly of  $2 \cdot C_{60}$  complexes: The  $C_{60}$  molecules (black spheres) are situated between the molecules of **2** approximately on top of the 3-cyanophenyl groups; the arrows indicate the major and minor growth directions. Reproduced with permission from ref 51. Copyright 2004 Wiley-VCH Verlag GmbH & Co. KGaA.

$C_{60}$  to form new highly organized and atomically well-defined functional materials (Figure 9). At room temperature, fullerenes jump from pore to pore with a rate of  $\sim 10^{-3} \text{ s}^{-1}$  at low coverages (0.01 ML). At higher coverages (0.02 ML),  $C_{60}$  molecules condense, forming supramolecular islands located close to empty porous areas. This finding has been accounted for by the attractive cohesive intermolecular interactions between the fullerene molecules.

However, not all of the 2D supramolecular ensembles obtained by deposition of porphyrins on surfaces yield the same results. Yokoyama and co-workers have described the formation of a flexible porous network upon adsorption of  $C_{60}$  on a Au(111) surface covered with a compact monolayer of porphyrin **4** (Figure 10) bearing two carboxylic groups.<sup>52</sup> In this case, it is the adsorption of  $C_{60}$  molecules that leads to the formation of nanopore structures by laterally shifting the supramolecular wires of porphyrins, which occurs simultaneously to the partial change in the conformation of the metalloporphyrin (Figure 10). A similar reorganization of the underlying molecular patterns has been observed for  $C_{60}$ /acridine 9-carboxylic acid (ACA) on Ag(111).<sup>53</sup>

Donor–acceptor 2D supramolecular ensembles have also been formed employing adsorbed shape-persistent macrocycles as surface templates. Thus, Freyland and co-workers have recently generated a 2D supramolecular structure from macrocycle **5** and its codeposition with fullerenes on HOPG (Figure 11).<sup>54</sup> STM images recorded under ambient conditions have been claimed to show that **5** is organized into rows separated by the interdigitated alkyl chains on the graphite surface. Further deposition of  $5/C_{60}$  in a 1:4 ratio

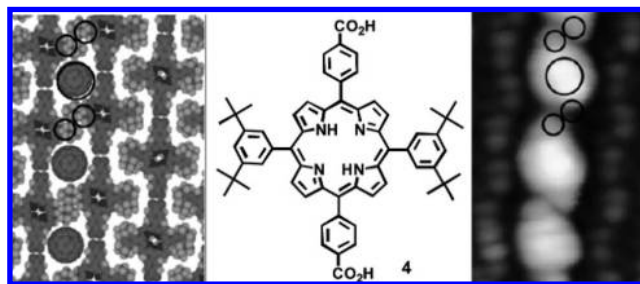


**Figure 10.** (a) Proposed model, chemical structure, and high-resolution STM image of a linear  $C_{60}$  chain arranged on self-assembled porphyrin **4**. The circles indicate the rotation of the porphyrin aryl substituents to avoid steric hindrance. Reproduced with permission from ref 52. Copyright 2007 Wiley-VCH Verlag GmbH & Co. KGaA.

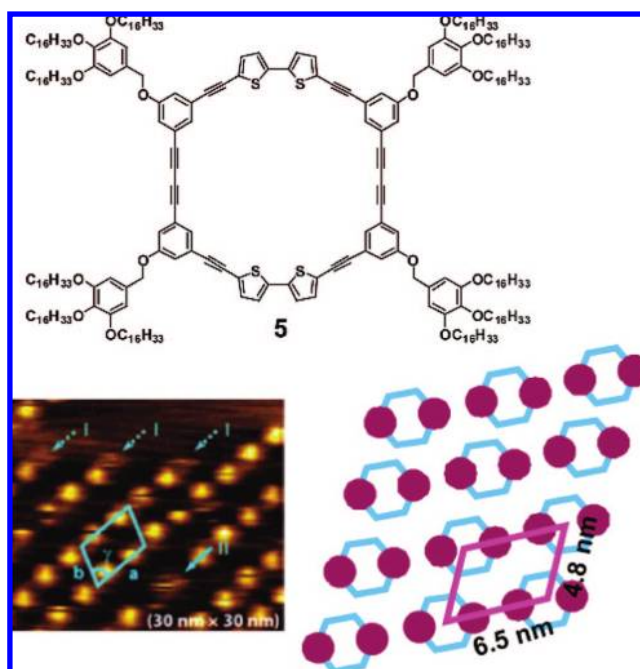


**Figure 11.** Chemical structure of macrocycle **5**, higher resolution STM image under ambient conditions, revealing the adsorption site of  $C_{60}$  on the macrocycle ( $V_{\text{bias}} = 1.0 \text{ V}$ , and  $I_t = 0.3 \text{ nA}$ ) and proposed structural model. Reproduced with permission from ref 54. Copyright 2006 American Chemical Society.

formed an array of well-ordered bright spots corresponding to two  $C_{60}$  molecules weakly bonded to the macrocycle. Each  $C_{60}$  pair is not located above the center of the macrocycle (intrinsic hole) but just on the two bithiophene moieties present in the macrocycle. Therefore, the driving force for this superstructure is not the interaction of the  $C_{60}$  units with the uncovered graphite surface inside the rings but the donor–acceptor interactions between the electron-rich bithiophene fragments and the electron-poor  $C_{60}$  molecule.

Cyclooligothiophene **6** (Figure 12) has also been reported to host  $C_{60}$  molecules on HOPG.<sup>55</sup> The packing of the macrocycles on the surface brings the ring-shaped  $\pi$ -systems together to distances of 0.4 nm, forming a “spiderlike” conformation, which allows the intermolecular interactions between the alkyl chains. These van der Waals interactions are the driving force for the self-organization of alkylated conjugated systems. The so-formed modified surface of ring-shaped  $\pi$ -type organic semiconductors is appropriately organized for complexing  $C_{60}$ . Thus, stable 1:1 host–guest complexes are formed. At very low coverage, different adsorption sites are observed, with the fullerene unit adsorbed

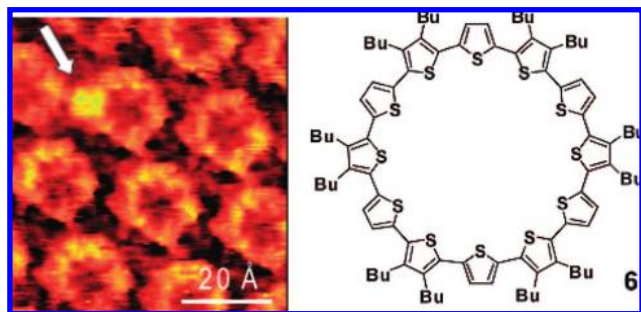


**Figure 12.** STM image (left) of a monolayer of cyclooligothiophene **6** on HOPG, including a  $6 \cdot C_{60}$  complex (white arrow). Image area,  $11.6 \times 8.7 \text{ nm}^2$ ; tunnelling conditions,  $V_{\text{bias}} = -700 \text{ mV}$ , and  $I_t = 44 \text{ pA}$ . Reproduced with permission from ref 55. Copyright 2002 Wiley-VCH Verlag GmbH & Co. KGaA.

in the cavity of the macrocycle or in the rim. Interestingly, at higher coverages (98%), the formation of multiple complexes involving more than one  $C_{60}$  molecule per oligothiophene is not observed, forming exclusively 1:1 complexes. The complexed fullerenes form a 2D crystalline superstructure exhibiting a true epitaxial growth matching the underlying macrocycle monolayer (Figure 12).

All of the examples hitherto described consist of hierarchically organized close-packed arrays of molecules on top of which subsequently deposited fullerenes sit. A different scenario is that of open nanoporous networks held by directional interactions, such as hydrogen bonding or metal coordination, whose pores act as nucleation sites for  $C_{60}$  adsorption. A representative example is the honeycomb structure resulting from codeposition of melamine and perylene tetracarboxylic diimide (PTCDI) on  $1 \text{ ML Ag-Si}(111) \sqrt{3} \times \sqrt{3} R 30^\circ$  surface.<sup>56</sup> Melamine can bind three PTCDI molecules through triple hydrogen bonds, along three axes forming an angle of  $120^\circ$  with each other. These hydrogen bonds direct the growth of a honeycomb structure whose nodes are melamine molecules linked by PTCDI molecules. Upon  $C_{60}$  deposition on this honeycomb structure,  $C_{60}$  adsorbs exclusively on the hexagonal nanopores of the honeycomb. Moreover, because of the particular size of the pore for the melamine-PTCDI network, it can accommodate seven  $C_{60}$  molecules and no more, and so,  $C_{60}$  heptamers can be found on the images. Following a similar approach with terphenyl and benzoic carboxylic acid molecules, which form nanoporous coordination networks upon codeposition with Fe, Stepanow et al. were able to probe that the  $C_{60}$  cluster size can indeed be controlled by the pore size, which, in turn, is determined by the size and shape of the molecular species that form the organic pattern.<sup>57</sup>

Stepanow et al. have also recently carried out a systematic STM study of the hierarchical self-assembly of Fe atoms and trimesic acid molecules (TMA, compound a in Figure 13) on a Cu(100) substrate in ultrahigh vacuum, forming broad-branched X-shape nanocavities with an opening of  $\sim 1 \text{ nm}$ . Each single nanocavity was formed by eight TMA molecules, and the structure that resulted was stable at temperatures as high as 500 K under vacuum conditions.<sup>58</sup> Fullerene  $C_{60}$  was further deposited on the nanocavity-covered substrate by thermal sublimation (690 K) from organic beam evaporators under UHV conditions, and the STM measurements were performed in situ at room temperature.

Figure 13e shows that each nanocavity binds only one fullerene  $C_{60}$  molecule. The apparent height of the adsorbed

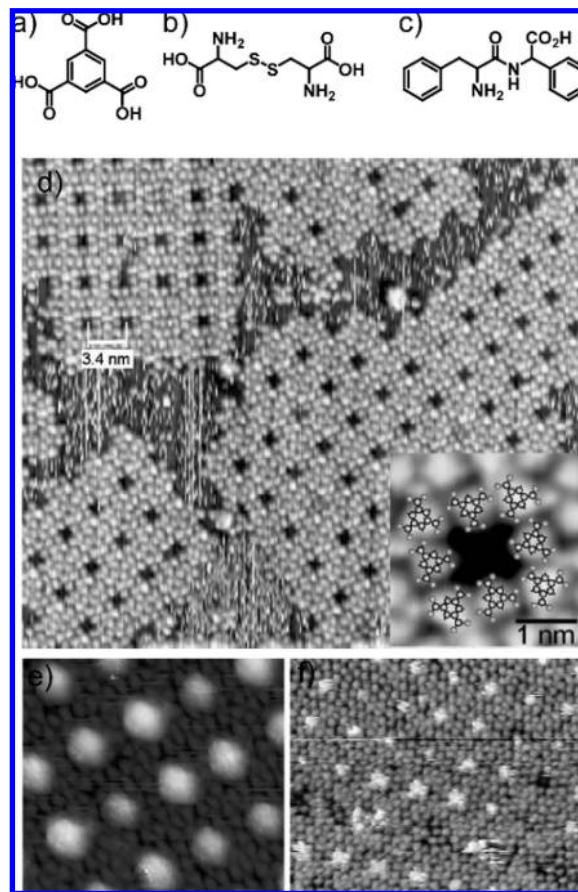


**Figure 13.** Chemical structures of trimesic acid (TMA, a), cystine (b), and Phe-Phe (c). (d) STM image (left) of the 2D metallosupramolecular nanocavities obtained on a Cu(100) substrate by hierarchical assembly of TMA and Fe atoms. The inset in panel d shows the proposed model for a single nanocavity surrounded by eight uncoordinated carboxylate groups. (e) STM images,  $14 \times 14 \text{ nm}^2$ , of the  $C_{60}$  binding in the receptors. The different molecular heights might reflect distinct adsorption configurations. (f) STM images,  $25 \times 22 \text{ nm}^2$ , of the Phe-Phe binding molecules in the receptors. Reproduced with permission from ref 58. Copyright 2006 Royal Society of Chemistry.

$C_{60}$  molecules is a result of the different configurations (orientation or position). In any case, adsorption of fullerene molecules was observed at the Cu surface, thus occurring exclusively at the nanocavities. To estimate the binding strength of the hierarchical organization, annealing experiments were performed. At 470 K, release of  $C_{60}$  was observed, this temperature being significantly lower than that required for the desorption of  $C_{60}$  from clean Cu surfaces [730 K for Cu(110)].<sup>59</sup> These STM experiments reveal the reversibility of the process, which is an important issue for the fabrication of 2D nanoarrays of fullerenes at solid surfaces.

#### 4. Coadsorbed Fullerene Systems and the Formation of Intermixed Layers at a Nanometer Scale

One step further in the construction of molecular self-assembled devices is the use of coadsorbed systems, which offer even broader possibilities for structure and property control.<sup>60</sup> In these systems, it has been shown that the adlayer structures formed depend on the ratio of the molecular components and their degree of coverage, resulting in a variety of different molecular structures.<sup>51,61</sup>

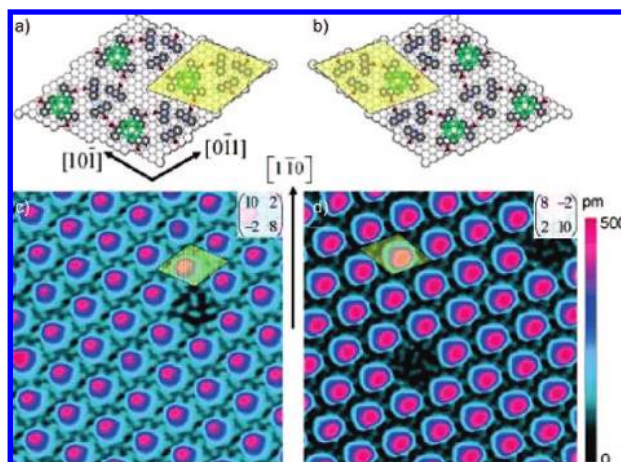


**Figure 14.** (a and b) Proposed models and STM images of the intermixed  $C_{60}$ -ACA supramolecular structures for the R and S chiral surfaces (c and d). A unit cell is indicated in each panel for reference purposes, along with the matrix notation of the domain. Reproduced with permission from ref 53. Copyright 2005 American Chemical Society.

As an outstanding example of the above concepts, Williams et al. have shown, by using a coadsorbed system formed by acridine-9-carboxylic acid (ACA) and fullerene  $C_{60}$  on Ag(111), that the formation of the intermixed structures depends on the balance between  $C_{60}$ -ACA-Ag(111) interactions.<sup>62</sup> Thus, upon changing the initial ACA coverage, two different  $C_{60}$ :ACA cooperative structures were formed (a chiral intermixed structure and a chainlike  $C_{60}$  structure). The chiral  $C_{60}$ :ACA structure was obtained at critical local coverage of 0.4 ML of ACA, whereas the chain  $C_{60}$ :ACA structure was related with a ACA dimer phase. Thus, important organization patterns, such as chirality or 1D chains, can be tuned as a function of the coverage of the predeposited ACA structures.

Chirality is a concept that has fascinated chemists from its very beginning, which has been used by Mother Nature for the construction of biologically active molecules, which, eventually, gave place to life. In this regard, the development of chirality on surfaces opens the way to an alternative procedure for the preparation of new chiral compounds and enantioselective reactions. Furthermore, chiral surfaces show enantiospecific properties of interest, such as, for instance, electron–molecule interactions,<sup>63</sup> polarization-dependent photoemission,<sup>64</sup> and nonlinear optical response.<sup>65</sup>

Chiral surfaces have been achieved by following two different strategies: (i) adsorption of chiral molecules on an achiral surface (direct-transfer chirality) and (ii) adsorption of achiral molecules, which became chiral when confined on a solid surface due to the symmetry breaking imposed by the surface (surface-confined chirality).<sup>53</sup> It is important to note, however, that in this second case, even though the adsorbed molecules become chiral, the surface phase often remains achiral due to the formation of the racemate. Fullerene  $C_{60}$  because of its  $I_h$  symmetry is not a good candidate for chiral symmetry breaking. However, as stated above, Williams et al. have shown that when coadsorbed with symmetric ACA ( $C_{2v}$  symmetry) on an epitaxially ordered Ag(111) surface, they form a chiral phase (Figure 14).<sup>53</sup>

In a recent study, we have carried out the growth of a self-assembled lateral superlattice of 2-[9-(1,3-dithiol-2-ylidene)anthracen-10(9*H*)-ylidene]-1,3-dithiole (exTTF, **7**)<sup>66</sup>

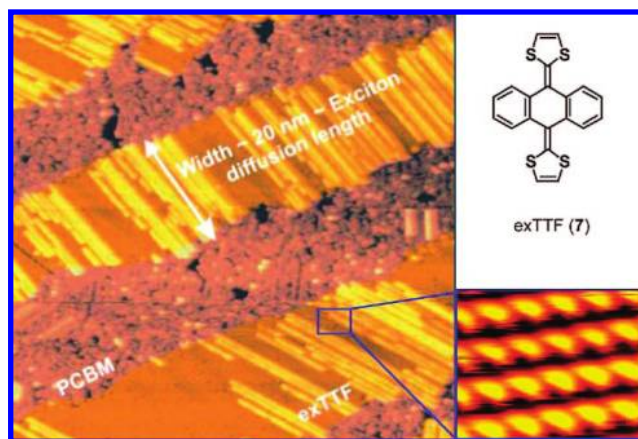


**Figure 15.** Nanoscale segregation of PCBM and exTTF mixtures on Au(111) ( $118 \times 132 \text{ nm}^2$ ). The inset shows the grow morphology of the ex-TTF films at  $\sim 1$  ML of coverage on Au(111). Reproduced with permission from ref 67. Copyright 2007 American Chemical Society.

as an electron donor and PCBM as an electron acceptor on Au(111) under UHV conditions at variable temperature. The superlattice areas were determined to be 10–20 nm in width (Figure 15).<sup>67</sup> The aim of this work was to use the nanometer-scale pattern provided by the well-known  $22 \times \sqrt{3}$  “herringbone” reconstruction of Au(111) surface as a template to steer the growth of the molecular species into 1D molecular nanostructures with sizes in good agreement with the exciton diffusion lengths (10–20 nm), as required for highly efficient photovoltaic solar cells.<sup>68</sup> Our results reveal that the lateral segregation of donor/acceptor blends into a long-range ordered superlattice where the appropriate morphology is feasible.

PCBM, which upon vacuum deposition on Au(111) leads to a coverage-dependent transition from substrate-controlled to (weak) H-bond-controlled self-assembly (see Figure 5),<sup>36</sup> and **7** were deposited from two separate glass crucibles resistively heated at 400 and 500 K, respectively, onto the Au(111) substrate, which was held at room temperature. Addition of  $\sim 0.6$  ML of **7** on top of the PCBM-based nanoscale spider-web structure results in the formation of two distinct areas observed by STM at room temperature: (i) a well-ordered area of exTTF where the elbow-free herringbone reconstruction underneath can be recognized as a long-period corrugation of the molecular rows and (ii) a disordered area reminiscent of the high-coverage PCBM phase.

This singular nanoscale phase segregation has been accounted for by (i) the low tendency of **7** and PCBM to mix, (ii) the high mobility of PCBM molecules at room temperature (used in the experiment), and (iii) the stronger interaction of **7** with the gold surface, in contrast to PCBM, which behaves as a 2D gas. Thus, the morphology and phase separation remain almost intact upon increasing the coverage, forming exTTF and PCBM stripes of around 20 nm, which compares well with typical exciton diffusion lengths.<sup>40,68</sup> These morphological features fulfill the requirements for the construction at the nanometer scale of efficient photovoltaic solar cells, and in a broader sense, they are of interest for the study of other optoelectronic devices where morphology between photo- and electro-active donor and acceptor species plays a leading role.

A well-ordered organic donor/acceptor nanojunction array formed by self-assembly of fullerene  $C_{60}$  (as an electron

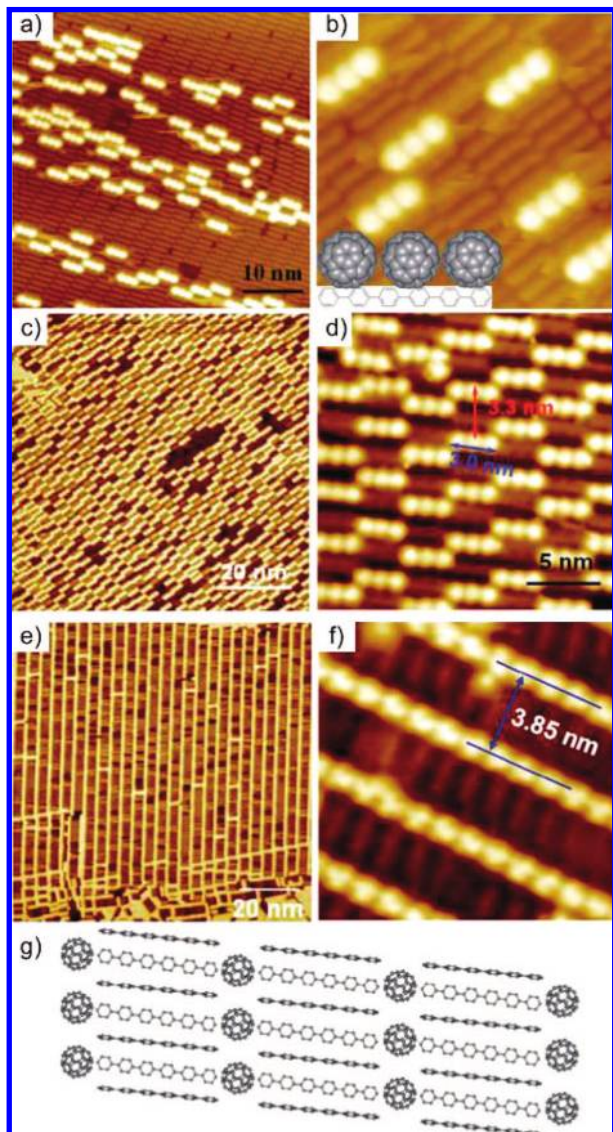


**Figure 16.** STM images [ $50 \times 50 \text{ nm}^2$  (a) and  $15 \times 15 \text{ nm}^2$  (b)] of 0.1 ML  $\text{C}_{60}$  on “face-on + edge-on” 6P layer on Ag(111) corresponding to the preferential adsorption of  $\text{C}_{60}$  triplets atop single 6P molecule. The inset in panel b shows the proposed model. STM images [ $80 \times 80 \text{ nm}^2$  (c) and  $20 \times 20 \text{ nm}^2$  (d)] of 0.5 ML  $\text{C}_{60}$  on face-on + edge-on 6P layer on Ag(111) showing the formation of a well-ordered vertical  $\text{C}_{60}/6\text{P}$  array. STM images [ $100 \times 100 \text{ nm}^2$  (e) and  $13 \times 13 \text{ nm}^2$  (f)] of the lateral  $\text{C}_{60}/6\text{P}$  arrays. (g) Schematic model for the regular superlattice of alternating  $\text{C}_{60}$  and 6P linear chains. Reproduced with permission from ref 69. Copyright 2008 American Physical Society.

acceptor) on the molecular nanotemplate formed by nanostripes of *p*-sexiphenyl (6P) (as an electron donor) on Ag(111) has recently been reported by Chen et al.<sup>69</sup> In this case, STM studies reveal the formation of  $\text{C}_{60}/6\text{P}$  arrays with a well-defined 2D arrangement. A further annealing process on the molecular superstructure formed by the  $\text{C}_{60}/6\text{P}$  at 380 K leads to the insertion of  $\text{C}_{60}$  linear chains between the 6P nanostripes, thus resulting in the formation of a periodic lateral nanostructure constituted by  $\text{C}_{60}$  and 6P molecules (Figure 16).

The examples collected in this section clearly reveal that the preparation of well-organized organic donor/acceptor nanojunction arrays is feasible as shown in the low-temperature STM investigations carried out on different donors (exTTFs, 6P) and  $\text{C}_{60}$  as a paradigmatic case of

electron acceptor molecule. These new 2D organic nanostructures represent outstanding and alternative realistic possibilities for the preparation of nanoelectronic devices.

## 5. Outlook

Although fullerenes have already been used for the direct coverage of different metal substrates from the very beginning, only recently they have been mixed with other appealing molecules, which nicely complement them from a geometric and electronic point of view. As a result, organic molecules previously deposited on a substrate have been used as new templates for the formation of 2D-ordered fullerene superstructures. Thus, planar as well as concave host organic molecules, namely, involving macrocycles, have been successfully used to accommodate fullerenes ( $\text{C}_{60}$  and  $\text{C}_{70}$ ) and fullerene derivatives in which the presence of alkyl chains or functional groups has a strong impact on the induced order. The different strategies followed along this review clearly show that the modification of the metal surface can be avoided by first decorating the solid surface with suitable organic molecules acting as templates and can be exploited in the construction of hierarchical assemblies of fullerene arrays. Furthermore, the rational design of coadsorbed systems results in outstanding achievements such as the generation of chiral surfaces, also described for other classes of organic molecules, or the organization of intermixed layers of electron donor and acceptor components. These 2D superlattices are thus new scenarios for testing, for instance, nonconventional enantiomeric synthesis (chiral surface) or unraveling the fundamental electron transfer process in intermixed layers for the production of optoelectronic devices at a nanometer scale. In summary, fullerenes—probably the most studied molecules during the last 20 years—are called to play a leading role in the development of 2D supramolecular organizations formed by the assembly of pristine and chemically modified fullerenes that can preserve the outstanding chemical, electrochemical, and photophysical properties that they exhibit.

## 6. Acknowledgments

Our own work has been supported by the MEC of Spain (MSR-FIS2007-0126, NAN-2004-08881-002-01, CTQ2004-00039/BQU, CTQ2008-00795/BQU, and CTQ2006-08558), Comunidad de Madrid (Nanomagnet S-0505/MAT/0194 and Madrisolar P-PPQ-000225-0505), and CONSOLIDER-INGENIO 2010 on Molecular Nanoscience (CSD2007-00010). R.O. thanks the Spanish Ministry for Science and Innovation for salary support.

## 7. References

- (1) (a) Special Issue on Organic Electronics. *Chem. Mater.* **2004**, *16*, 4381. (b) Wassel, R. A.; Gorman, C. B. *Angew. Chem., Int. Ed.* **2004**, *43*, 5120. (c) Carroll, R. L.; Gorman, C. B. *Angew. Chem., Int. Ed.* **2002**, *41*, 4378. (d) Whitesides, G. M. *Small* **2005**, *1*, 172. (e) Balzani, V. *Small* **2005**, *1*, 278.
- (2) Heimel, G.; Romaner, L.; Zojer, E.; Bredas, J.-L. *Acc. Chem. Res.* **2008**, *41*, 721.
- (3) (a) Daniel, M.-C.; Astruc, D. *Chem. Rev.* **2004**, *104*, 293. (b) Thomas, G.; Kamat, P. V. *Acc. Chem. Res.* **2003**, *36*, 888.
- (4) Murray, R. W. *Chem. Rev.* **2008**, *108*, 2688.
- (5) Zotti, G.; Vercelli, B.; Berlin, A. *Acc. Chem. Res.* **2008**, *41*, 1098.
- (6) Shirai, Y.; Morin, J.-F.; Sasaki, T.; Guerrero, J. M.; Tour, J. M. *Chem. Soc. Rev.* **2006**, *35*, 1043.
- (7) (a) Astruc, D.; Ornelas, C.; Ruiz, J. *Acc. Chem. Res.* **2008**, *41*, 841. (b) Hwang, S.-H.; Moorefield, C. N.; Newkome, G. R. *Chem. Soc. Rev.* **2008**, *37*, 2543.

- (8) Kamat, P. V. *J. Phys. Chem. C* **2007**, *111*, 2834.
- (9) Zabet-Khosousi, A.; Dhirani, A.-A. *Chem. Rev.* **2008**, *108*, 4072.
- (10) Tour, J. M. *J. Org. Chem.* **2007**, *72*, 7477.
- (11) (a) For SAMs involving fullerenes, see Bonifazi, D.; Enger, O.; Diederich, F. *Chem. Soc. Rev.* **2007**, *36*, 390. (b) For the organization of fullerenes in supramolecular structures by means of ionic and nonionic forces based on the amphiphilic character of the fullerene derivatives, see Guldi, D. M.; Zerbetto, F.; Georgiakilas, V.; Prato, M. *Acc. Chem. Res.* **2005**, *38*, 38.
- (12) Martín, N. *Chem. Commun.* **2006**, 209, 3.
- (13) (a) Hirsch, A. *The Chemistry of Fullerenes*; Wiley-VCH: Weinheim, Germany, 2005. (b) Guldi, D. M.; Martín, N. *Fullerenes: From Synthesis to Optoelectronic Properties*; Kluwer Academic Publishers: Dordrecht, The Netherlands, 2002. (c) Langa, F.; Nierengarten, J.-F. *Fullerenes: Principles and Applications*; RSC Publishing: Cambridge, United Kingdom, 2007.
- (14) Special issue on Supramolecular Chemistry of Fullerenes. Martín, N.; Nierengarten, J.-F., Eds. *Tetrahedron* **2006**, *62*, 1905.
- (15) (a) Barth, J. V.; Constantini, G.; Kern, K. *Nature* **2005**, *437*, 671. (b) Lu, W.; Lieber, C. M. *Nat. Mater.* **2007**, *6*, 841.
- (16) (a) De Feyter, S.; De Schryver, F. C. *Chem. Soc. Rev.* **2003**, *32*, 139. (b) Wan, L.-J. *Acc. Chem. Res.* **2006**, *39*, 334.
- (17) (a) Barth, J. V.; Weckesser, J.; Cai, C.; Günter, P.; Bürgi, L.; Jeandupeux, O.; Kern, K. *Angew. Chem., Int. Ed.* **2000**, *39*, 1230. (b) Theobald, J. A.; Oxtoby, N. S.; Phillips, M. A.; Champness, N. R.; Beton, P. H. *Nature* **2003**, *424*, 1029. (c) Otero, R.; Schök, M.; Molina, M. L.; Lægsgaard, E.; Hammer, B. B.; Besenbacher, F. *Angew. Chem., Int. Ed.* **2005**, *44*, 2270.
- (18) Tamai, A.; Seitsonen, A. P.; Baumberger, F.; Hengsberger, M.; Shen, Z.-X.; Greber, T.; Osterwalder, J. *Phys. Rev. B* **2008**, *77*, 075134.
- (19) Silien, C.; Pradhan, N. A.; Ho, W.; Thiry, P. A. *Phys. Rev. B* **2004**, *69*, 115434.
- (20) Lu, X.; Grobis, M.; Khoo, K. H.; Louie, S. G.; Crommie, M. F. *Phys. Rev. B* **2004**, *70*, 115418.
- (21) (a) Wang, L.-L.; Cheng, H.-P. *Phys. Rev. B* **2004**, *69*, 045404. (b) Wang, L.-L.; Cheng, H.-P. *Phys. Rev. B* **2004**, *69*, 165417.
- (22) Modesti, S.; Cerasari, S.; Rudolf, P. *Phys. Rev. Lett.* **1993**, *71*, 2469.
- (23) Weckesser, J.; Cepek, C.; Fasel, R.; Barth, J. V.; Baumberger, F.; Greber, T.; Kern, K. *J. Chem. Phys.* **2001**, *115*, 9001.
- (24) Murray, P. W.; Pedersen, M. Ø.; Lægsgaard, E.; Stensgaard, I.; Besenbacher, F. *Phys. Rev. B* **1997**, *55*, 9360.
- (25) Pedersen, M. Ø.; Murray, P. W.; Lægsgaard, E.; Stensgaard, I.; Besenbacher, F. *Surf. Sci.* **1997**, *389*, 300.
- (26) Abel, M.; Dmitriev, A.; Fasel, R.; Lin, N.; Barth, J. V.; Kern, K. *Phys. Rev. B* **2003**, *67*, 245407.
- (27) Hinterstain, M.; Torrelles, X.; Felici, R.; Rius, J.; Huang, M.; Fabris, S.; Fuess, H.; Pedio, M. *Phys. Rev. B* **2008**, *77*, 153412.
- (28) Cepek, C.; Fasel, R.; Sancrotti, M.; Greber, T.; Osterwalder, J. *Phys. Rev. B* **2001**, *63*, 125406.
- (29) Pai, W. W.; Hsu, C.-L.; Lin, M. C.; Lin, K. C.; Tang, T. B. *Phys. Rev. B* **2004**, *69*, 125405.
- (30) Zhang, X.; Yin, F.; Palmer, R. E.; Guo, Q. *Surf. Sci.* **2008**, *602*, 885.
- (31) Altman, E. I.; Colton, R. J. *J. Vac. Sci. Technol. B* **1994**, *12*, 1906.
- (32) Barth, J. V.; Brune, H.; Ertl, G.; Behm, R. J. *Phys. Rev. B* **1990**, *42*, 9307.
- (33) Brune, H.; Giovanni, M.; Bromann, K.; Kern, K. *Nature* **1998**, *394*, 451.
- (34) Chambliss, D. D.; Wilson, R. J.; Chiang, S. *Phys. Rev. Lett.* **1991**, *66*, 1721.
- (35) Hummelen, J. C.; Knight, B. W.; LePeq, F.; Wudl, F.; Yao, J.; Wilkins, C. L. *J. Org. Chem.* **1995**, *60*, 532.
- (36) Écija, D.; Otero, R.; Sánchez, L.; Gallego, J. M.; Wang, Y.; Alcamí, M.; Martín, F.; Martín, N.; Miranda, R. *Angew. Chem., Int. Ed.* **2007**, *46*, 7874.
- (37) (a) Altman, E. I.; Colton, R. J. *Surf. Sci.* **1992**, *279*, 49. (b) Fujita, D.; Yakabe, T.; Nejoh, H.; Sato, T.; Iwatsuki, M. *Surf. Sci.* **1996**, *366*, 93.
- (38) Xiao, W.; Ruffieux, P.; Ait-Mansour, K.; Gröning, O.; Palotas, K.; Hofer, W. A.; Gröning, P.; Fasel, R. *J. Phys. Chem. B* **2006**, *110*, 21394.
- (39) Néel, N.; Kröger, J.; Berndt, R. *Appl. Phys. Lett.* **2006**, *88*, 163101.
- (40) For recent reviews on organic solar cells, see (a) Brabec, C. J.; Sariciftci, N. S.; Hummelen, J. C. *Adv. Funct. Mater.* **2001**, *11*, 15. (b) Coakley, K. M.; McGehee, M. D. *Chem. Mater.* **2004**, *16*, 4533. (c) Günes, S.; Neugebauer, H. *Chem. Rev.* **2007**, *107*, 1324. (d) Armaroli, N.; Balzani, V. *Angew. Chem., Int. Ed.* **2007**, *46*, 52. (e) Thompson, B. C.; Fréchet, J. M. J. *Angew. Chem., Int. Ed.* **2008**, *47*, 58. (f) Balzani, V.; Credi, A.; Venturi, M. *ChemSusChem* **2008**, *1*, 26.
- (41) Desiraju, G. R. *Chem. Commun.* **2005**, 2995.
- (42) Nakanishi, T.; Miyashita, N.; Michinobu, T.; Wakayama, Y.; Tsuruoka, T.; Ariga, K.; Kurth, D. G. *J. Am. Chem. Soc.* **2006**, *128*, 6328.
- (43) Deak, D. S.; Silly, F.; Porfyrakis, K.; Castell, M. R. *J. Am. Chem. Soc.* **2006**, *128*, 13976.
- (44) Deak, D. S.; Porfyrakis, K.; Castell, M. R. *Chem. Commun.* **2007**, 2941.
- (45) Altman, E. I.; Colton, R. J. *Phys. Rev. B* **1993**, *48*, 18244.
- (46) Hashizume, T.; Motai, K.; Wang, X. D.; Shinohara, H.; Saito, Y.; Maruyama, Y.; Ohno, K.; Kawazoe, Y.; Nishina, Y.; Pickering, H. W.; Kuk, Y.; Sakurai, T. *Phys. Rev. Lett.* **1993**, *71*, 2959.
- (47) Gimzewski, J. K.; Modesti, S.; David, T.; Schlittler, R. R. *J. Vac. Sci. Technol. B* **1994**, *12*, 1942.
- (48) Schull, G.; Berndt, R. *Phys. Rev. Lett.* **2007**, *99*, 226105.
- (49) Pan, G.-B.; Liu, J.-M.; Zhang, H.-M.; Wan, L.-J.; Zheng, Q.-Y.; Bai, Ch.-L. *Angew. Chem., Int. Ed.* **2003**, *42*, 2747.
- (50) For recent examples on the complexation of C<sub>60</sub> and porphyrins in solution, see (a) Nobukuni, H.; Shimazaki, Y.; Tani, F.; Naruta, Y. *Angew. Chem., Int. Ed.* **2007**, *46*, 8975. (b) Yanagisawa, M.; Tashiro, K.; Yamasaki, M.; Aida, T. *J. Am. Chem. Soc.* **2007**, *129*, 11912.
- (51) Bonifazi, D.; Spillmann, H.; Kiebele, A.; de Wild, M.; Seiler, P.; Cheng, F.; Güntherodt, H.-J.; Jung, T.; Diederich, F. *Angew. Chem., Int. Ed.* **2004**, *43*, 4759.
- (52) Nishiyama, F.; Yokohama, T.; Kamikado, T.; Yokoyama, S.; Mashiko, S.; Sakaguchi, K.; Kikuchi, K. *Adv. Mater.* **2007**, *19*, 117.
- (53) Xu, B.; Tao, C.; Cullen, W. G.; Reutt-Robey, J. E.; Williams, E. D. *Nano Lett.* **2005**, *11*, 2207.
- (54) Pan, G.-B.; Cheng, X.-H.; Cogger, S.; Freyland, W. *J. Am. Chem. Soc.* **2006**, *128*, 4218.
- (55) (a) Mena-Osteritz, E.; Bäuerle, P. *Adv. Mater.* **2006**, *18*, 447. (b) Mena-Osteritz, E. *Adv. Mater.* **2002**, *14*, 609.
- (56) Swarbrick, J. C.; Rogers, B. L.; Champness, N. R.; Beton, P. H. *J. Phys. Chem. B* **2006**, *110*, 6110.
- (57) Stepanow, S.; Lingenfelder, M.; Dmitriev, A.; Spillmann, H.; Delvigne, E.; Lin, N.; Deng, X.; Cai, C.; Barth, J. V.; Kern, K. *Nat. Mater.* **2004**, *3*, 229.
- (58) Stepanow, S.; Lin, N.; Barth, J. V.; Kern, K. *Chem. Commun.* **2006**, 2153.
- (59) Fasel, R.; Agostino, R. G.; Aebi, P.; Schlapbach, L. *Phys. Rev. B* **1999**, *60*, 4517.
- (60) (a) Theobald, J. A.; Oxtoby, N. S.; Phillips, M. A.; Champness, N. R.; Beton, P. H. *Nature* **2003**, *424*, 1029. (b) Yoshimoto, S.; Higa, N.; Itaya, K. *J. Am. Chem. Soc.* **2004**, *126*, 8540. (c) Suto, K.; Yoshimoto, S.; Itayot, K. *J. Am. Chem. Soc.* **2003**, *125*, 14976. (d) Pan, G. B.; Liu, J. M.; Zhang, H. M.; Wan, L. J.; Zheng, Q. Y.; Bai, C. L. *Angew. Chem., Int. Ed.* **2003**, *42*, 2747.
- (61) (a) Griessl, S. J. H.; Lackinger, M.; Jamitzky, F.; Markert, T.; Hietschold, M.; Heckl, W. A. *Langmuir* **2004**, *20*, 9403. (b) de Wild, M.; Berner, S.; Suzuki, H.; Yanagi, H.; Schlettwein, D.; Ivan, S.; Barattoff, A.; Guentherodt, H. J.; Jung, T. A. *ChemPhysChem* **2002**, *3*, 881.
- (62) Xu, B.; Tao, C.; Williams, E. D.; Reutt-Robey, J. E. *J. Am. Chem. Soc.* **2006**, *128*, 8493.
- (63) Ray, K.; Ananthavel, S. P.; Waldeck, D. H.; Naaman, R. *Science* **1999**, *283*, 814.
- (64) Polcik, M.; Allegretti, F.; Sayago, D. I.; Nisbet, G.; Lamont, C. L. A.; Woodruff, D. P. *Phys. Rev. Lett.* **2004**, *92*, 236103.
- (65) Verbiest, T.; Van Elshocht, S.; Kauranen, M.; Hellemans, L.; Snauwaert, J.; Nuckolls, C.; Katz, T. J.; Persoons, A. *Science* **1998**, *282*, 913.
- (66) (a) Yamashita, Y.; Kobayashi, Y.; Miyashi, T. *Angew. Chem., Int. Ed. Engl.* **1989**, *28*, 1052. (b) Bryce, M. R.; Moore, A. J.; Hasan, M.; Ashwell, G. J.; Fraser, A. T.; Clegg, W.; Hursthouse, M. B.; Karaulov, A. I. *Angew. Chem., Int. Ed. Engl.* **1990**, *29*, 1450. (c) Martín, N.; Sánchez, L.; Seoane, C.; Ortí, E.; Viruela, P. M. *J. Org. Chem.* **1998**, *63*, 1268. (d) Segura, J. L.; Martín, N. *Angew. Chem., Int. Ed.* **2001**, *40*, 1372. (e) Martín, N.; Sánchez, L.; Herranz, M. A.; Illescas, B.; Guldi, D. M. *Acc. Chem. Res.* **2007**, *40*, 1015.
- (67) Otero, R.; Écija, D.; Fernández, G.; Gallego, J. M.; Sánchez, L.; Martín, N.; Miranda, R. *Nano Lett.* **2007**, *7*, 2602.
- (68) (a) Choong, V.; Park, Y.; Gao, Y.; Wehrmeister; Müllen, K.; Hsieh, B. R.; Tang, C. W. *Appl. Phys. Lett.* **1996**, *69*, 1492. (b) Halls, J. J. M.; Pichler, K.; Friend, R. H.; Moratti, S. C.; Holmes, A. B. *Appl. Phys. Lett.* **1996**, *68*, 3120.
- (69) Chen, W.; Zhang, H. L.; Huang, H.; Chen, L.; Shen Wee, A. T. *Appl. Phys. Lett.* **2008**, *92*, 193301.